

Work of the non-linear force within the D3, CD5 model

Before discussing the transfer within D3, CD5 model we present some appreciable numerical results within the model and their comparison with observational data. As it was shown theoretically in D3 and CD5, the non-linear (NL) interactions are crucial for the mesoscale dynamics and observational effects. An analogous conclusion was drawn by Chelton et al. (2011) from the analysis of observational data: “*essentially all of the observed mesoscales features are non-linear*” including mesoscale eddies which “*do not move with the mean velocity but with their own drift velocity*”. This conclusion agrees with the observation of Richardson (1993) that mesoscale eddies are “*water-mass anomalies that have nearly circular flow around their centers and that survive for many rotations and may move through the background water at speeds and directions inconsistent with background flow*” The C11 observational result for the drift velocity is in agreement with the earlier theoretical predictions of D3 and CD5 (see, Canuto et al., 2017a). In Canuto et al. (2017b) are presented also other theoretical results of D3 and CD5 which are determined by NL interactions and compared favorably with observational data. In Fig.1 borrowed from Canuto et al. (2017a), we present the comparison of the predicted drift velocity with observational data which were obtained later (Fu, 2009; Chelton and Schlax, 2013). In D3 and CD5 we parameterized the NL terms of the dynamical mesoscale equations on the basis of the general approach to modeling NL interactions in turbulent flows developed by the authors before (see the list of those articles in the manuscript under the discussion). Some validations of D3, CD5 are demonstrated below in Figs.1-3 borrowed from the submitted papers by Canuto et al. (2017a,b). The NL mesoscale dynamics radically modifies the transformation of EPE and EKE in comparison with the results of the linear analysis presented in the quoted above Vallis’s text book. In particular, consider Eq.(5.7) of the manuscript under discussion which yields the EKE production $P_K(r_d)$ by EPE at scales of the deformation radius r_d :

$$P_K(r_d) = -2r_d^{-1}K^{3/2} < 0 \quad (\text{a})$$

where K is EKE. The mesoscale characteristics K and r_d demonstrate the fact that $P_K(r_d)$ is due to the cascades, i.e. due to the NL interaction. The negative sign in Eq.(a) means that at scales $\sim r_d$ EKE transforms into EPE. In fact, EKE is produced by the a-geostrophic component of the velocity \mathbf{u}_a . In Fourier space we have:

$$P_k(\mathbf{k}) = -\text{Im}\left[p_*(\mathbf{k})\mathbf{k} \cdot \mathbf{u}_a^*(\mathbf{k})\right] \quad (\text{b})$$

where $p = \rho_0 p_*$ is the pressure, $\rho_0 = 10^3 \text{ kg/m}^3$ is the reference density. In the case of a small $Ro(k)$ from the referred above equations of D3 or CD5 to the main order of EKE using the manuscript notations we deduce:

$$\mathbf{u}_a(\mathbf{k}) = -Ro(k)\mathbf{e}_z \times \mathbf{u}_g(\mathbf{k}), \quad f\mathbf{e}_z \times \mathbf{u}_g(\mathbf{k}) = -ikp_* \quad (\text{c})$$

where \mathbf{e}_z is the unit vertical vector, f is the Coriolis parameter. From Eqs.(b), (c) we get

$$P_k(\mathbf{k}) = -k^2 f^{-1} Ro(k) |p_*(\mathbf{k})|^2 < 0 \quad (\text{d})$$

i.e. at small $Ro(k)$ EKE transforms into EPE but not vice versa. It is worth recalling that this result is obtained with account for the negative turbulent viscosity in the referred mesoscale equations which, in turn, is due to the inverse energy cascade created by NL interactions which is absent in the linear approximation. In the opposite case of a large $Ro(k)$ the effect of rotation is weak and the velocity equation yields the usual EPE \rightarrow EKE conversion.

References

Canuto, V.M. and. Dubovikov, M.S., 2005 Modeling mesoscale eddies, *Ocean Model.*, **8**, 1-30, cited CD5.

Canuto, V.M., Y. Cheng, M.S.Dubovikov, A.M. Howard, 2017a Parameterization of mixed layer and deep ocean mesoscales including non-linearity, , *J. Phys. Oceanogr.*, submitted after revision.

Canuto, V.M., Y. Cheng, M.S.Dubovikov, A.M. Howard, 2017b Mesoscale diffusivity: a location and depth dependent model. *J. Phys. Oceanogr.*, to be submitted.

Chelton, D.B., M.G.Schlx and R.M.Samelson, 2011 Global observations of non-linear mesoscale eddies, *Progress in Oceanography*, **91**, 167-216

Dubovikov, M.S., 2003 Dynamical model of mesoscale eddies. *Geophys. Astrophys Fluid Dyn.*, **7**, 311-358.

Fu, L.L., 2009, Patterns and velocity of propagation of the global ocean eddy variability. *J.Geophys.Res.*, **114**, C11017, doi:10.1029/2009JC005349.

Kraichnan, R.H., 1975 Statistical dynamics of two-dimensional flow. *J. Fluid Mech.*, **67**, 155-171.

Muller, P., J. McWilliams, and Molemaker, 2005 Routes to Dissipation the Ocean: The 2D/3D Turbulence Conundrum. In H. Baurmert, J. Simpson, and J. Sundermann, editors, *Marine Turbulence – Theories, Observations and Models. Results of the CARTUM Project*. Cambridge Press.

Phillips, H.E. and S.R.Rintoul, 2000 Eddy variability and energetics from direct measurements in the ACC south of Australia, *J. Phys. Oceanogr.*, **30**, 3050-3076

Richardson, P.L., 1993 Tracking ocean eddies, *American Scientist*, **81**, 261-271.

Scott, R.B. and Arbic, B.K., 2007 Spectral energy fluxes in geostrophic turbulence: implications for ocean energetics. *J. Phys. Oceanogr.*, **37**, 673-688.

Scott, R.B. and Wang, F., 2005 Direct evidence of an oceanic inverse kinetic energy cascade from satellite altimetry. *J. Phys. Oceanogr.*, **35**, 1650-1666.

Smith, K.S. and J.Marshall, 2009 Evidence for enhanced eddy mixing at middepth in the Southern Ocean, *J. Phys. Oceanogr.*, **39**, 50-69

WOCE Data Products Committee, 2002, WOCE Global Data, Version 3.0, WOCE International Project Office, WOCE Report No. 180/02, Southampton, UK.

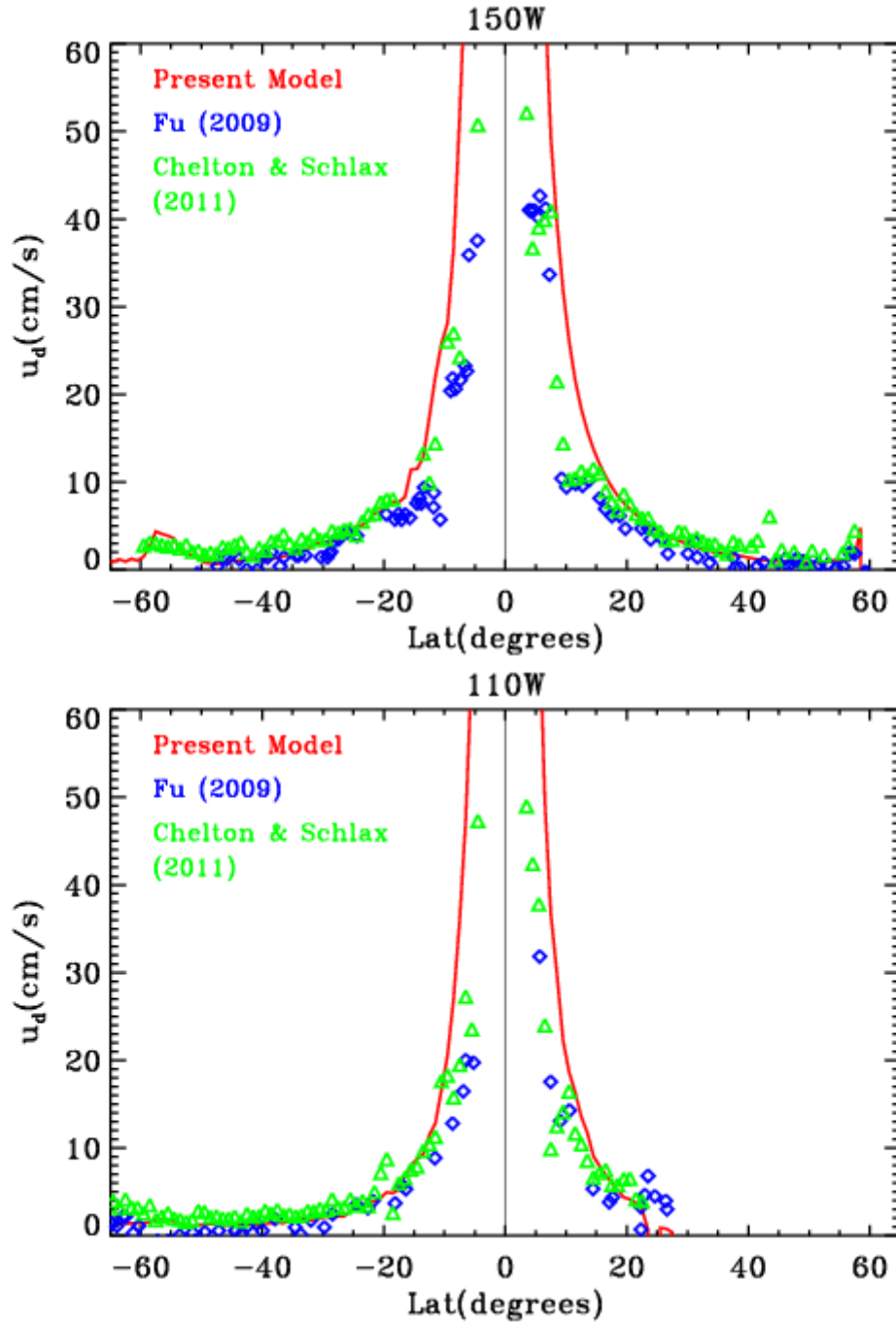


Fig.1. Borrowed from Canuto et al. (2017a). Comparison of $|\mathbf{u}_d|$ derived in D3 and CD5 with the data of Fu (2009) and Chelton and Schlax (2011) at 150°W and 110°W . The data are reproduced satisfactorily. In all the figures, the model results were obtained from an average of the last 3 years of a simulation with the GISS ER stand-alone OGCM which was run for 300 years.

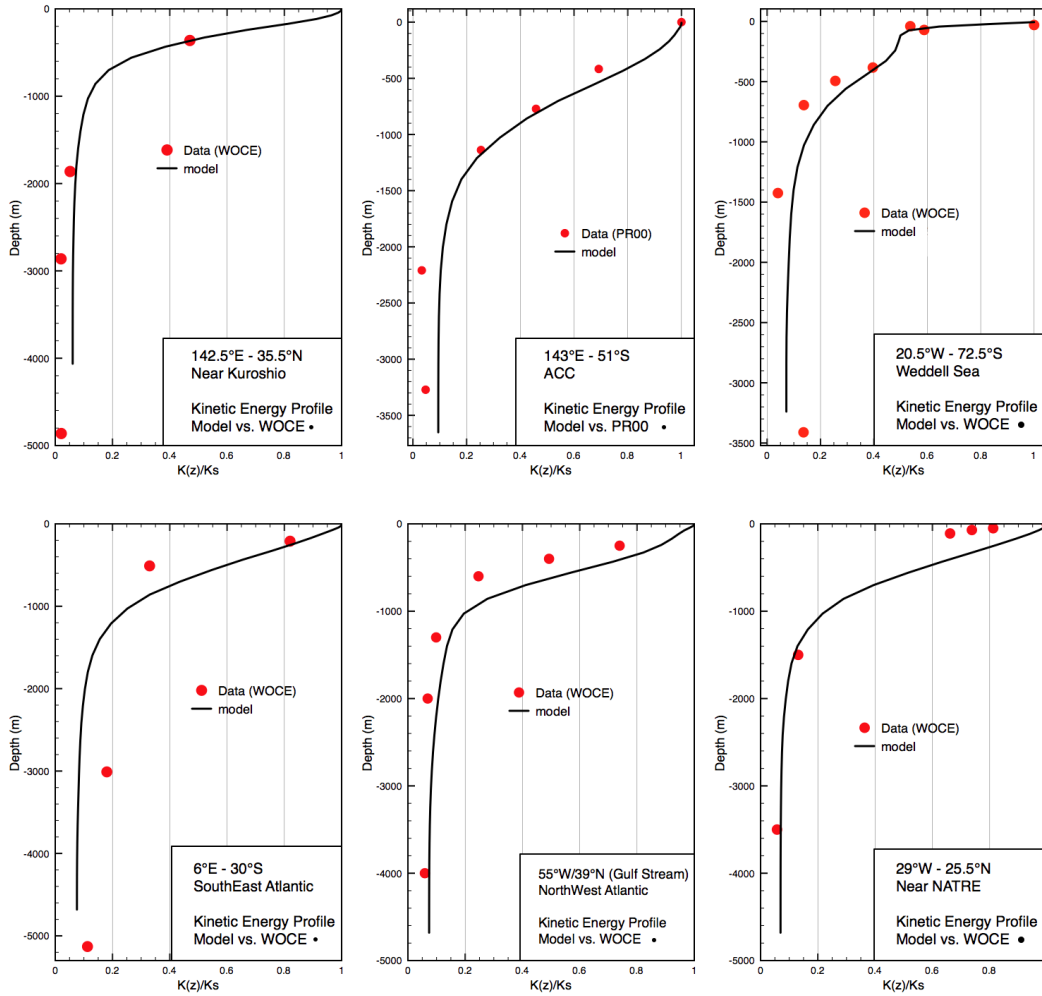


Fig.2. Borrowed from Canuto et al. (2017b). Comparison of the z-profile of the EKE derived in d3 and CD5 in units of its surface value vs. WOCE data in different locations. The model results reproduce the data satisfactorily.

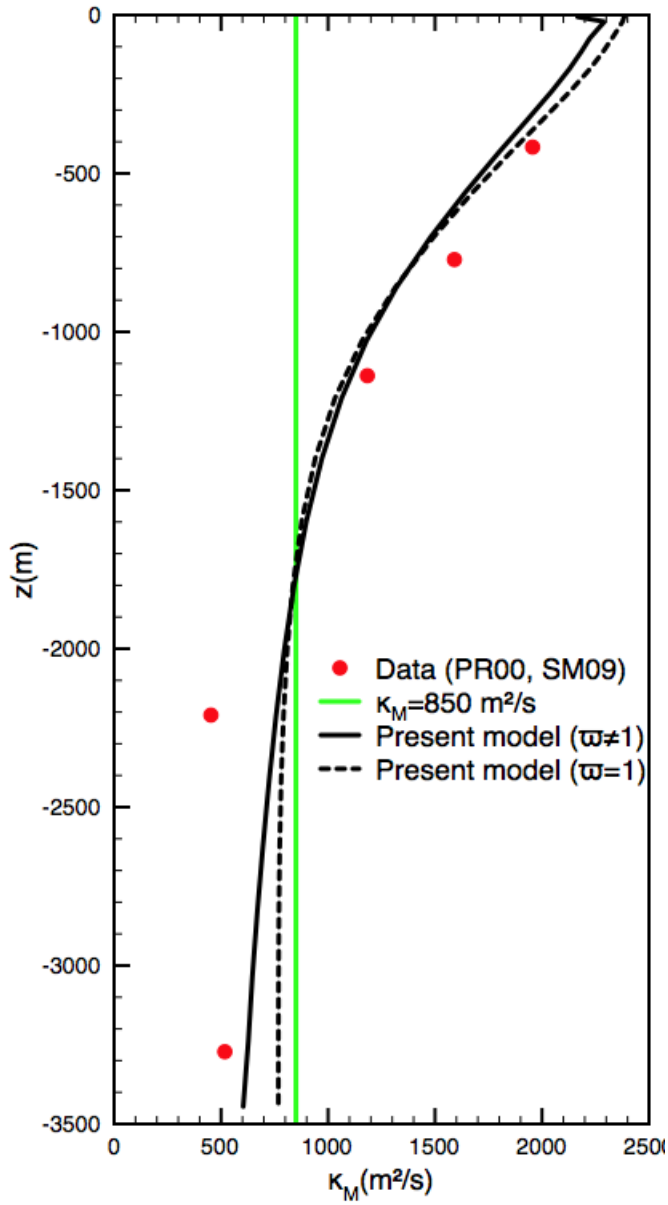


Fig.3 Borrowed from Canuto et al. (2017b). Comparison of mesoscale diffusivity (in m^2s^{-1}) computed within D3 and CD5 model vs. the measured data of Philips and Rintoul (2000, PR00) in the ACC (143E, 51S). The $\varpi=1$ case is with the contribution of corrections of the higher order in the small parameter equal to the ratio (mean K/EKE).